

Constraints on changes in fundamental constants from a cosmologically distant OH absorber/emitter

N. Kanekar^{1,*}, C. L. Carilli¹, G. I. Langston¹, G. Rocha², F. Combes³,
R. Subrahmanyan⁴, J. T. Stocke⁵, K. M. Menten⁶, F. H. Briggs^{4,7}, and T. Wiklind^{8,9}
¹National Radio Astronomy Observatory, USA; ²Cavendish Laboratory, UK; ³Observatoire de Paris,
France; ⁴Australia Telescope National Facility, Australia; ⁵University of Colorado,
USA; ⁶Max-Planck-Institut für Radioastronomie, Germany; ⁷Australian National University,
Australia; ⁸Space Telescope Science Institute, USA; ⁹Onsala Space Observatory, Sweden
(Dated: December 2, 2024)

We have detected the four 18cm OH lines from the $z \sim 0.765$ gravitational lens toward PMN J0134–0931. The 1612 and 1720 MHz lines are in conjugate absorption and emission, providing a laboratory to test the evolution of fundamental constants over a large lookback time. We compare the HI and OH main-line absorption redshifts of the different components in the $z \sim 0.765$ absorber and the $z \sim 0.685$ lens toward B0218+357 to place stringent constraints on changes in $F \equiv g_p [\alpha^2/\mu]^{1.57}$. We obtain $[\Delta F/F] = (0.44 \pm 0.36^{\text{stat}} \pm 1.0^{\text{synt}}) \times 10^{-5}$, consistent with no changes in these constants over the redshift range $0 < z < 0.7$. The measurements have a 2σ sensitivity of $[\Delta\alpha/\alpha] < 6.7 \times 10^{-6}$ and $[\Delta\mu/\mu] < 1.4 \times 10^{-5}$ to fractional changes in α and μ , over a period of ~ 6.5 Gyr, half the age of the Universe. These are among the most sensitive current constraints on changes in μ .

PACS numbers: 98.80.Es, 06.20.Jr, 33.20.Bx, 98.58.-w

Introduction.— A fairly generic feature of modern higher-dimensional theoretical models (such as Kaluza-Klein and superstring theories) is that fundamental constants like the fine structure constant α , the electron-proton mass ratio $\mu \equiv m_e/m_p$, the proton gyromagnetic ratio g_p , etc, depend on the scale lengths of the extra dimensions of the theory. In the current theoretical framework, it is implausible that these scale lengths remain constant, implying that quantities like α , μ , etc should vary with time. The detection of such changes provides an avenue to probe new and fundamental physics.

Null results have been obtained in all terrestrial studies of evolving constants, with atomic clocks and isotopic abundances in the Oklo natural fission reactor providing the tightest constraints on fractional changes in the fine structure constant ($(1/\alpha) [\Delta\alpha/\Delta t] < 4 \times 10^{-15}$ per year, over three years [1], and $\Delta\alpha/\alpha < 1.2 \times 10^{-7}$, over $\sim 1.8 \times 10^9$ years [2], respectively). However, these and other terrestrial measurements probe fairly small fractions of the age of the Universe; astrophysical techniques are needed to examine the possibility that fundamental constants might have varied at earlier times (e.g. [3, 4, 5, 6, 7]). It is these techniques, involving a comparison between the measured frequencies of different spectral transitions arising in the same cosmologically distant object, that have provided tantalizing evidence for changes in α (e.g. [3]). The most recent result, using the “many-multiplet” method with Keck telescope optical spectra, gives $\Delta\alpha/\alpha = (-5.4 \pm 1.2) \times 10^{-6}$ over the redshift range $0.2 < z < 3.7$ [3]. However, a similar technique, applied to Very Large Telescope spectra, yields a conflicting result, $\Delta\alpha/\alpha = (-0.6 \pm 0.6) \times 10^{-6}$, over $0.4 < z < 2.3$ [4]. Independent techniques are clearly needed as systematics do appear to play a significant role in the current results.

Redshifted radio OH lines provide a new method to estimate changes in α , μ and g_p [8, 9, 10]. The four 18cm OH

lines have very different dependences on these constants and their redshifted frequencies can hence be compared to measure any variation. Comparisons between the redshifts of main OH lines (at 1665.4018 and 1667.3590 MHz) and those of the HI 21cm hyperfine line or HCO⁺ rotational lines can be used to provide an independent measure of any changes in these constants (e.g. [11]). Even more interesting is the case of conjugate emission/absorption by the 18cm satellite OH lines, detected in a single cosmologically distant object (at $z \sim 0.247$ toward PKS1413+135; [5, 12]). Here, the pumping mechanism guarantees that the two lines arise from the same gas; a comparison can thus be made between the 1720 and 1612 MHz redshifts without concerns about systematic motions between the clouds in which the different lines arise.

A problem with the OH technique is that only four redshifted OH main absorbers are currently known [13, 14, 15], with high resolution data only available for the $z \sim 0.685$ lens toward B0218+357 [15]. Similarly, only one redshifted conjugate OH satellite system is known, at a relatively low redshift, $z \sim 0.247$; this corresponds to a lookback time of ~ 2.9 Gyr, not much earlier than the time range probed by the Oklo reactor [26]. We report here the detection of all four 18cm OH lines in a new absorption/emission system at $z \sim 0.765$, corresponding to a lookback time of ~ 6.7 Gyr.

Spectra and results— The redshifted OH 18cm lines from the $z \sim 0.765$ lens toward PMN J0134–0931 were observed simultaneously with the Green Bank Telescope (GBT) in October, 2004, and January, 2005, with an observing resolution of ~ 1 km/s (after Hanning smoothing). A separate GBT observation in January, 2005, provided a high resolution spectrum in the redshifted HI 21cm line, originally detected by [16]. The HI 21cm and main-line OH spectra (smoothed to resolutions of ~ 5 and ~ 14.5 km/s, respectively, and resampled) are shown in Figs. 1[A] and [B], while the three pan-

els of Fig. 2 show the 1720 and 1612 MHz satellite spectra and the sum of 1720 and 1612 MHz optical depths (all after smoothing to, and resampling at, a resolution of ~ 4.7 km/s). PMN J0134–0931 is unresolved by the GBT beam; the optical depths shown in the figures are the ratio of line flux density to measured total continuum flux density for each transition (using the low optical depth limit). All spectra have an optical depth RMS noise of ~ 0.0018 , per ~ 5 km/s channel.

Besides the above, the redshifted HCO^+ 2–1 line was observed with the IRAM 30m telescope and the Australia Telescope Compact Array, the 6 cm ground state H_2CO doublet lines with the GBT and, finally, the 2 cm first rotationally excited state H_2CO lines with the Very Large Array and the GBT. None of these transitions were detected, down to 3σ optical depth limits of $\tau < 0.07$ for the HCO^+ line and $\tau < 0.002$, $\tau < 0.005$ for the ground and excited state H_2CO lines, respectively. This is curious as every other redshifted molecular absorber has been detected in both HCO^+ and OH absorption (e.g. [13, 14, 17, 18]). While the structure of the background source is very different at the frequencies of the HCO^+ and OH lines, implying that small-scale structure in the molecular cloud could be an issue, it is still surprising that none of the OH components, at very different velocities from each other, show any trace of mm-wave absorption.

The HI 21cm profile has three fairly clear components, two of which are blended and well-separated from the third. Similarly, both the 1667 and 1665 MHz OH lines show two clearly resolved components, with the lower redshift one somewhat asymmetric, suggesting that it is blended. While the redshifts of the two strong 21cm and main OH components are similar, the OH satellite lines are blue-shifted by ~ 10 km/s relative to the lowest redshift (highest frequency) component in Fig. 1[A] and [B]. This is reminiscent of the situation in the other redshifted conjugate OH system, PKS1413+135 [5]. In both cases, the sum of the satellite frequencies is different from the sum of the main line frequencies; since the two sums have the same dependence on α , μ and g_p [8, 9], the satellite and main OH lines must arise in different gas.

The bottom panel of Fig. 2 shows that the sum of the 1720 and 1612 MHz optical depths is consistent with noise; the satellite lines are thus conjugate with each other. Such conjugate behavior arises due to competition between the intra-ladder 119μ and cross-ladder 79μ decay routes to the OH ground state, after the molecules have been pumped by collisions or far-infra-red radiation into the higher excited states [19, 20]. The fact that the 1720 MHz line is seen in emission and the 1612 MHz, in absorption, implies that the intra-ladder decay route dominates. This, and the requirement that the 119μ transition be optically thick for the 1720 MHz line to be inverted [20], yields the constraint $3.5 \times 10^{15} \lesssim N_{\text{OH}} \lesssim 3.5 \times 10^{16} \text{ cm}^{-2}$ on the OH column density.

The luminosity in the 1720 MHz line is $L_{\text{OH}} \sim 3700L_{\odot}$, making this the brightest known 1720 MHz megamaser by more than an order of magnitude. It is also the most distant OH megamaser, by a factor of three in redshift; for comparison, the furthest known 1667 MHz megamaser is at $z \sim 0.265$

[21]. This is also the first case of conjugate OH satellite emission/absorption in a “normal” galaxy; all previous cases were objects containing an active galactic nucleus (e.g. Cen A, NGC1052, PKS1413+135; [5, 20, 22]), where the OH level populations might have been affected by nuclear activity. This is very interesting as it suggests that such conjugate emission/absorption might not be as rare as earlier expected and hence, that it might be used as a tool to probe both spatial and temporal changes in fundamental constants.

Constraining changes in fundamental constants.— A comparison between the redshifts of different spectral lines to measure changes in fundamental constants involves the assumption that the lines have no intrinsic velocity offsets from each other. Note that this is true even for comparisons between lines of the same species as different transitions might be excited under different physical conditions and thus, in different spatial locations. This appears to be the case with the main and satellite OH lines here, implying that one cannot compare their redshifts to estimate changes in the different constants.

However, as emphasized in [5, 12] for the case of PKS1413+135, the conjugate nature of the satellite lines ensures that they arise in the same physical region and, crucially, that systematic velocity offsets are not an issue. The different dependences of the sum and difference of the 1720 MHz and 1612 MHz frequencies on α , μ and g_p then allows us to estimate changes in the quantity $G \equiv g_p [\alpha^2/\mu]^{1.85}$ [5, 8]. The low signal-to-noise ratio of the 1720 and 1612 spectra of Fig. 2 precludes such an estimate at the present time; however, the high redshift of the system implies that it is an excellent target for deep integrations in the satellite lines and should thus provide a precision measurement of changes in the different constants in the future. For example, high resolution observations with the Square Kilometer Array, a next generation radio telescope, should be able to detect fractional changes $\Delta G/G \sim 5 \times 10^{-7}$ in this system, implying a sensitivity of $\sim 1.4 \times 10^{-7}$ to changes in $\Delta\alpha/\alpha$. This is similar to the sensitivity of the Oklo measurement but with fewer assumptions and out to a far larger lookback time of ~ 6.7 Gyr. In addition, this sensitivity would be obtained from a single system, unlike the many-multiplet method, which requires a large number of absorbers to average out systematic effects. A comparison between the results from the conjugate systems in PKS1413+135 [5] and PMN J0134–0931 will thus allow one to probe true spatio-temporal changes in the above constants (instead of merely averaging over spatial effects), especially since the two sources are very widely separated on the sky.

Comparisons between the HI 21cm and main OH lines suffer from the drawback of possible systematic velocity offsets between the two species, implying that individual spectral components might have significant redshift differences. However, a tight correlation has been found between the velocities of HCO^+ and nearest HI 21cm absorption in the Galaxy, with a dispersion of only ~ 1.2 km/s [23]. Further, the velocities of Galactic OH and HCO^+ absorption have been found to be remarkably similar ([24]; see Figs. 4 and 5 of [24]). OH and

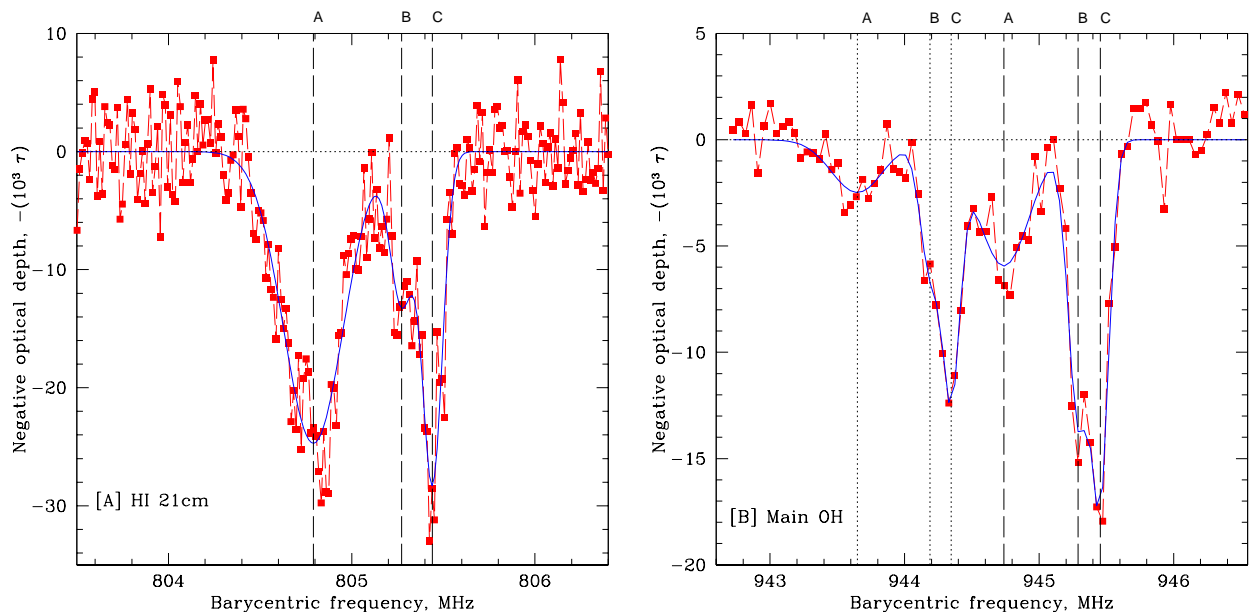


FIG. 1: GBT HI 21cm ([A], ~ 5 km/s resolution) and OH main line ([B], ~ 14.5 km/s resolution) spectra toward PMN J0134–0931, with negative optical depth ($-10^3 \times \tau$) plotted against barycentric frequency, in MHz. The solid line shows the three-gaussian fit to each spectrum. The vertical lines in each figure indicate the locations of the three components (marked A, B and C), with the dashed and dotted lines in [B] showing the 1667 and 1665 components, respectively.

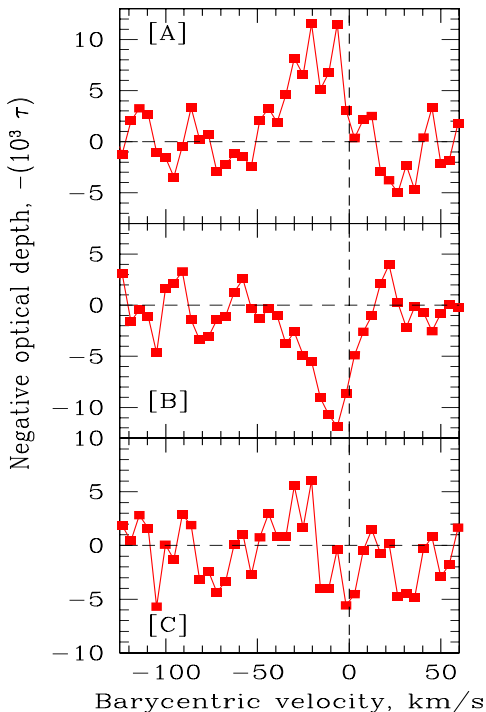


FIG. 2: OH satellite line spectra (~ 5 km/s resolution), with negative optical depth ($-10^3 \times \tau$) plotted against barycentric velocity, in km/s, relative to $z = 0.76355$, the redshift of component C. [A] 1720 MHz transition, redshifted to ~ 975.6 MHz; [B] 1612 MHz transition, redshifted to ~ 912.2 MHz; [C] Sum of 1612 and 1720 MHz spectra; this spectrum is consistent with noise. Note that the feature at ~ -30 km/s is not statistically significant. The satellite lines peak ~ 10 km/s blueward of component C (the dashed vertical line), which has the lowest redshift of the three spectral components.

HI 21cm velocities should thus also be well-correlated and, in fact, the dispersion in this correlation is likely to be less than that between the HCO^+ and HI 21 velocities, as the spatial structure of the background source is quite similar at the nearby OH 18 cm and HI 21cm frequencies. It should thus be possible to use a comparison between main OH and HI 21cm absorption from a statistically large number of redshifted systems as an independent probe of any evolution in the fundamental constants [8, 9]. We next apply this technique to the absorbers toward PMN J0134–0931 and B0218+357 [8], albeit using a more conservative dispersion of 3 km/s between OH and HI intrinsic velocities, characterising internal motions within a molecular cloud.

The HI 21cm profile of Fig. 1[A] has the highest signal-to-noise ratio of our spectra (at the same resampled resolution of ~ 1 km/s) and has three clear components. We hence used a three-gaussian template to locate the peak redshifts of the different 21cm absorption components, with the amplitudes, positions and widths of the gaussians all left as free parameters. A similar three-gaussian fit was then carried out to the smoothed and resampled 1665 and 1667 MHz spectra, with the difference that the velocity widths here were fixed to those obtained from the 21cm fit and only the amplitudes and positions of the individual components were left as free parameters. The 1665 and 1667 MHz fits were carried out simultaneously, to account for the possibility of blending between the components. We note that the original spectral resolution was ~ 1 km/s in all cases and no additional components were seen in any of the spectra. The possibility that strong narrow components might be blended in the lower resolution spectra of Figs. 1 [A] and [B] can thus be ruled out.

Figs. 1[A] and [B] show the fitted Gaussians as solid lines, overlaid on the HI and OH spectra. The three 21cm components have peak redshifts $z_{\text{HI-A}} = 0.764938 \pm 0.000015$, $z_{\text{HI-B}} = 0.763881 \pm 0.000033$ and $z_{\text{HI-C}} = 0.763515 \pm 0.000014$, from the three-gaussian fits. Similarly, the sum of the 1665 and 1667 MHz frequencies have peak redshifts $z_{\text{OH-A}} = 0.764871 \pm 0.000042$, $z_{\text{OH-B}} = 0.763852 \pm 0.000019$ and $z_{\text{OH-C}} = 0.763550 \pm 0.000010$. Comparing the above redshifts, component by component, we obtain $[\Delta F/F]_{\text{A}} = (-3.7 \pm 2.8) \times 10^{-5}$, $[\Delta F/F]_{\text{B}} = (-1.6 \pm 2.1) \times 10^{-5}$ and $[\Delta F/F]_{\text{C}} = (2.0 \pm 1.0) \times 10^{-5}$, where $F \equiv g_p [\alpha^2/\mu]^{1.57}$ and only statistical (i.e. measurement) errors have been included. A weighted average of these values gives $[\Delta F/F] = (0.86 \pm 0.86) \times 10^{-5}$. We note that a comparison using an entirely unconstrained six-Gaussian fit to the OH spectrum gives the weighted average $[\Delta F/F] = (2.25 \pm 0.84) \times 10^{-5}$. Similarly, the HI 21cm and main OH redshifts in the $z \sim 0.685$ lens toward B0218+357 are $z_{\text{HI}} = 0.684676 \pm 0.000005$ [25] and $z_{\text{OH}} = 0.684682 \pm 0.0000056$ [8], giving $[\Delta F/F]_{\text{D}} = (3.5 \pm 4.0) \times 10^{-6}$. All the above values are consistent with the null hypothesis of no evolution in the different constants. Combining results from the two absorbers (using the constrained fit and a weighted average), we obtain $[\Delta F/F] = (0.44 \pm 0.36^{\text{stat}} \pm 1^{\text{syst}}) \times 10^{-5}$, over $0 < z \lesssim 0.7$, where the second error is due to systematic velocity offsets between HI and OH lines which, as mentioned above, are estimated using a velocity dispersion of 3 km/s. Of course, four measurements are far too small for a reliable estimate of this error. However, the fact that the OH and HI redshifts are in reasonable agreement within the measurement errors in all four cases (two of which have measurement errors $\lesssim 1 \times 10^{-5}$) suggests that systematic velocity offsets do not dominate the accuracy of the measurement.

The strong dependence of F on α and μ ($F \propto \alpha^{3.14}$ and $F \propto \mu^{-1.57}$) implies a 2σ sensitivity of $[\Delta\alpha/\alpha] < 6.7 \times 10^{-6}$ and $[\Delta\mu/\mu] < 1.4 \times 10^{-5}$ to fractional changes in α and μ from $z \sim 0.7$ (i.e. a lookback time of ~ 6.5 Gyrs) to today, where we have added the errors in quadrature. Assuming a linear evolution model, these correspond to 2σ sensitivities of $(1/\alpha)[\Delta\alpha/\Delta t] < 1.1 \times 10^{-15} \text{ yr}^{-1}$ and $(1/\mu)[\Delta\mu/\Delta t] < 2.1 \times 10^{-15} \text{ yr}^{-1}$. These are among the best present constraints on changes in μ ; for comparison, [7] obtain $[\Delta\mu/\mu] < 1.48 \times 10^{-5}$ for $0 < z \lesssim 2.75$ and [6] obtain $[\Delta\mu/\mu] \lesssim 2 \times 10^{-5}$ for $0 < z < 2.0$, at 2σ level, using redshifted optical lines. We note that the present radio analysis is not affected by two important sources of systematic error in the optical regime (absolute wavelength calibration and relative isotopic abundances; e.g. [3]), although it should also be pointed out that the optical observations probe a larger redshift range. The primary source of the error in our technique is likely to lie in the velocity dispersion between OH and HI lines and perhaps in blending between weak narrow spectral components. As mentioned above, we do not feel that these dominate the present results; deeper observations in the redshifted OH and HI lines should help quantify their effects.

While the size of the radio sample is presently small, surveys are being carried out that will significantly increase the number of known redshifted OH, HI and HCO^+ absorbers. Further, the two conjugate OH satellite absorbers provide an excellent laboratory to investigate the true spatio-temporal evolution of the different constants. Comparisons between radio lines are thus likely to provide an important independent constraint on changes in fundamental constants in the future.

We thank Bob Garwood and Jim Braatz for help with the data analysis. The National Radio Astronomy Observatory is operated by Associated Universities, Inc., under cooperative agreement with the National Science Foundation. The Australia Telescope Compact Array is part of the Australia Telescope, funded by the Commonwealth of Australia for operation as a National Facility managed by CSIRO.

* Electronic address: nkanekar@aoc.nrao.edu

- [1] E. Peik, B. Lipphardt, H. Schnatz, T. Schneider, C. Tamm, and S. G. Karshenboim, *Phys. Rev. Lett.* **93**, 170801 (2004).
- [2] T. Damour and F. J. Dyson, *Nucl. Phys. B* **480**, 37 (1996).
- [3] M. T. Murphy, J. K. Webb, and V. V. Flambaum, *MNRAS* **345**, 609 (2003).
- [4] R. Srianand, H. Chand, P. Petitjean, and B. Aracil, *Phys. Rev. Lett.* **92**, 121302 (2004).
- [5] N. Kanekar, J. N. Chengalur, and T. Ghosh, *Phys. Rev. Lett.* **93**, 051302 (2004).
- [6] P. Tzanavaris, J. K. Webb, M. T. Murphy, V. V. Flambaum, and S. J. Curran, *Phys. Rev. Lett.* **95**, 041301 (2005).
- [7] A. Ivanchik et al., *A&A* **440**, 45 (2005).
- [8] J. N. Chengalur and N. Kanekar, *Phys. Rev. Lett.* **91**, 241302 (2003).
- [9] J. Darling, *Phys. Rev. Lett.* **91**, 011301 (2003).
- [10] N. Kanekar and J. N. Chengalur, *MNRAS* **350**, L17 (2004).
- [11] S. J. Curran, N. Kanekar, and J. Darling, *New Astr. Rev.* **48**, 1095 (2004).
- [12] J. Darling, *ApJ* **612**, 58 (2004).
- [13] J. N. Chengalur, A. G. de Bruyn, and D. Narasimha, *A&A* **343**, L79 (1999).
- [14] N. Kanekar and J. N. Chengalur, *A&A* **381**, L73 (2002).
- [15] N. Kanekar, J. N. Chengalur, A. G. de Bruyn, and D. Narasimha, *MNRAS* **345**, L7 (2003).
- [16] N. Kanekar and F. H. Briggs, *A&A* **412**, L29 (2003).
- [17] T. Wiklind and F. Combes, *A&A* **299**, 382 (1995).
- [18] T. Wiklind and F. Combes, *A&A* **328**, 48 (1997).
- [19] M. Elitzur, *Astronomical Masers*, Kluwer, Dordrecht, The Netherlands (1992).
- [20] H. J. van Langevelde, E. F. van Dishoek, M. N. Sevenster, and F. P. Israel, *ApJ* **448**, L123 (1995).
- [21] W. A. Baan, J. Rhoads, K. Fisher, D. R. Altschuler, and A. Haschik, *ApJ* **396**, L99 (1992).
- [22] R. C. Vermeulen, E. Ros, K. I. Kellermann, M. H. Cohen, J. A. Zensus, and H. J. van Langevelde, *A&A* **401**, 113 (2003).
- [23] M. J. Drinkwater, J. K. Webb, J. D. Barrow, and V. V. Flambaum, *MNRAS* **295**, 457 (1998).
- [24] H. Liszt and R. Lucas, *A&A* **355**, 333 (2000); H. Liszt, private communication (2005).
- [25] C. L. Carilli et al. *Phys. Rev. Lett.* **85**, 5511 (2000).
- [26] Throughout this paper, we use an LCDM cosmology, with $\Omega_m = 0.3$, $\Omega_\Lambda = 0.7$ and $H_0 = 70 \text{ km/s/Mpc}^{-1}$.